Khan *et al. Micro and Nano Systems Letters* (2023) 11:24
https://doi.org/10.1186/s40486-023-00187-6

Micro and Nano Systems Letters

LETTER

Open Access

Synthesis and optoelectronic properties of an anthracene derivative

Darya Khan[1], Zhang Xiaotao[1*], Muhammad Hasnain Jameel[2*], Mohd Arif Bin Agam[2], Muhammad Sufi Bin Roslan[2] and Majed A. Bajaber[3]

Abstract

An asymmetric a-side alkyl chain anthracene derivative 6-(4 (-2 Ethyl Octyl) Phenyl) 2Phenyl Anthracene (EOPPA) was designed based on a π-electron skeleton with a side alkyl chain of anthracene core molecule. EOPPA was found to be a sturdy and high-performance p-type semiconductor for optoelectronic applications. The creation has successfully made this new material EOPPA with the best solubility, which exhibits both sufficient solvent solubility and thermal stability. The asymmetrical structural features of EOPPA allowed for the preparation of two-dimensional crystalline thin films in micrometer sizes with 100 nm thicknesses on a Si/SiO_2 substrate through a solution processing method. The efficient solution processing synthesis of EOPPA and its high performance suggest that it has great potential in the field of organic electronics. The EOPPA demonstrated optoelectronic properties, crystalline structure, and good thin-film transistors having mobilities higher than 0.18 $cm^2 V^{-1} S^{-1}$, and a high current on/off ratio that can withstand temperatures of almost 225 °C. Furthermore, EOPPA presents good potential to be amongst the next generation of p-type anthracene core organic semiconductors, especially for practical printed electronics applications.

Keywords Organic semiconductors, Organic field-effect transistors, Alkyl chain, Conductivity, Crystallinity

Introduction

Organic semiconductors are mostly applied in the fields of organic field effect transistors (OFETs), organic solar cells (OSCs), and organic light-emitting diodes (OLEDs) [1, 2]. In recent years, there has been a substantial increase in interest in organic thin film transistors (OTFTs) and their usage in numerous technological applications [3–5]. It is required to find conjugated semiconductors with high mobility and strong environmental stability in order to fully realize the potential of these applications. P-type (hole-transporting), n-type (electron-transporting), and P/n-type bipolar semiconductors are some of the organic oligomers that have been researched so far [6, 7]. According to several research groups, pentacene has been used as a p-type semiconductor material with charge mobility of over 1.0 cm^2/V, and it has been found to have the highest charge carrier mobility in thin-film transistors [8]. However, Anthony's research group has reported solvable pentacene and anthracenedithioene derivatives with silylethynyl-substituent structures, despite poor stability and reproducibility limiting its commercial potential [9, 10].

Among the diverse organic semiconductor materials reported to date, Anthracene, an organic semiconductor material, has been a subject of ongoing research and modification since its first study of electrical conductivity in 1953 [1, 11, 12]. Furthermore, Anthracene's conjugated, rigid structure offers charge transport properties for field-effect transistors, but its

*Correspondence:
Zhang Xiaotao
zhangxt@tju.edu.cn
Muhammad Hasnain Jameel
mhasnainjamil@gmail.com
[1] Tianjin Key Laboratory of Molecular Optoelectronic Science, Department of Chemistry, Tianjin University, Tianjin 300072, China
[2] Faculty of Applied Sciences and Technology, University Tun Hussein Onn Malaysia, 86000 Batu Pahat, Malaysia
[3] Department of Physics, College of Sciences, Princess Nourah Bint Abdulrahman University (PNU), P.O. Box 84428, 11671 Riyadh, Saudi Arabia

small π-conjugation leads to poor field-effect behavior, resulting in only 0.02 $cm^2 V^{-1} S^{-1}$ mobility [13]. The enhanced π-stacking crystal packing has improved stability and charge mobility compared to the parent molecules [14–16]. Exploring molecular design strategies, such as designing large band gap semiconductor materials like anthracene derivatives, is a promising approach to improving the stability of organic semiconductors [17].

The studies developed a new p-type organic semiconductor, 2,6-bis(4-cyclohexyl phenyl)anthracene (DcHPA), by incorporating Cyclohexyl phenyl into the anthracene molecular skeleton at position 2,6 and systematically comparing its n-hexyl phenyl substituted compound, so the DnHPA's sublimation temperature decreases by 50 °C, and when heated to 80 °C, its mobility decreases by 50%, leading to rapid degradation and failure to function at 120 °C. Few studies have investigated the modification of anthracene derivatives with two-sided alkyl chains to create p-type molecules. Further investigation is required to determine the effects of molecular stacking and photoelectric properties using only one side chain [18–20]. So the decrease of π-conjugate systems in parent propylene provides another method to improve stability [21]. Due to their efficient molecular conjugation and molecular packing, the 2- or 2, 6-position anthracene derivatives are thought to be the most promising materials for application in anthracene derivative semiconductors [22].

For that achievement, we designed and synthesized a side alkyl chain anthracene derivative p-type organic semiconductor molecule, it is necessary to investigate how the alkyl chain on one side affects molecular stacking and its optoelectronic and physiochemical properties, thermal stability, solubility, and charge transfer characteristics. To report our recent discovery and improvement of a new P-type semiconductor material. The material has an asymmetrically substituted 2-Phenyl Anthracene backbone with 6-(4 (-2 Ethyl Octyl) Phenyl) groups as a side chain. Modify the molecular skeleton of the anthracene derivatives p-type semiconductor through the alkyl chain. The new molecule EOPPA showed strong optoelectronic properties, thermal stability, solubility, and mobility for thin film devices. These traits are in accordance with their molecular compositions and theoretical computations. The study provides valuable insights into designing and synthesizing p-type semiconductors from anthracene, considering the impact of electronic substituents. Based on the research, it appears that EOPPA has great potential for use in organic optoelectronics applications.

Experimental section

Materials and general methods

The reagents and chemicals were obtained from commercial sources and used as received without requiring additional purification. To synthesize EOPPA, the following steps were performed meticulously. use a dry 100 mL reaction flask with a stir bar and add 6(trifluoromethanesulfonate) 2phenyl anthracene (0.036 g or 0.74 mol), 4(2Etheyl Octyl) Phenylboronic acid pinacol ester phenyl boric acid (0.25 g or 0.74 mol), and tetra (triphenylphosphine) palladium as a catalyst Pd (pph3)4 (0.036 g or 0.32×10^{-4} mol). Vent the flask three times with argon (Ar) gas (0). Then 1–2 mL Ethanol, 9 mL toluene, and 1 M k_2CO_3 aqueous solution that had been degassed with nitrogen were added to the reaction flask. The mixture was stirred at 90 °C for 24 h. Once the reaction was complete, the mixture was filtered through a Celite pad and washed with CH_2Cl_2. The organic layer was then successfully washed with water, and the solvent was removed. The product was purified through column chromatography and sublimation techniques and followed by a sublimation of 5 h at 220 °C. Then 0.20 g (57.93%) of a yellowish solid was obtained. The ^{1}H NMR (600 MHz, CD_2Cl_2) δ (ppm) 8.51 (s, 1H), 8.47 and MS (EI): m/z 471 (M+). An analysis was conducted on C36H38 (Additional file 1: Fig. S1). The full synthetic and other relevant details can be found in Additional file 1.

The Bruker 400 and 600 Nuclear Magnetic Resonance (NMR) spectrometer was used to record the ^{1}H NMR spectra. The deuterated reagents used for EOPPA were (600 MHz, CD_2Cl_2) δ (d 0.00 ppm). Thermal gravimetric analysis curves (TGA) were obtained on a METTLER TOLEDO TGA apparatus with a heating rate of 10 °C min^{-1} in nitrogen. Ultraviolet-visible (UV–vis) spectra were measured on a SHI-MADZU UV-3600 UV–vis–NIR spectrophotometer (Japan). Cyclic voltammetry (CV) curves were scanned on a CHI660C electrochemistry station in dry CH_2Cl_2, tetrabutlyammonium hexafluorophosphate (Bu_4NPF_6) was used as an electrolyte (0.1 M) and ferrocene was used as an internal standard. Glassy carbon, Pt wire, and Ag/AgCl were used as the working, counter, and reference electrodes, respectively. The crystal structure and molecular packing of the EOPPA material were analyzed to study the influence of substituents on its structure using X-ray diffraction, selected area electron diffraction (SAED), and Transmission electron microscopy (TEM) technical. X-ray diffraction (XRD) measurement was performed in reflection mode at 40 kV and 200 mA with Cu Ka radiation using a 2 kW Rigaku D/max-2500, XRD, TEM, and SAED measurements were carried out on a JEM 1011 (Japan).

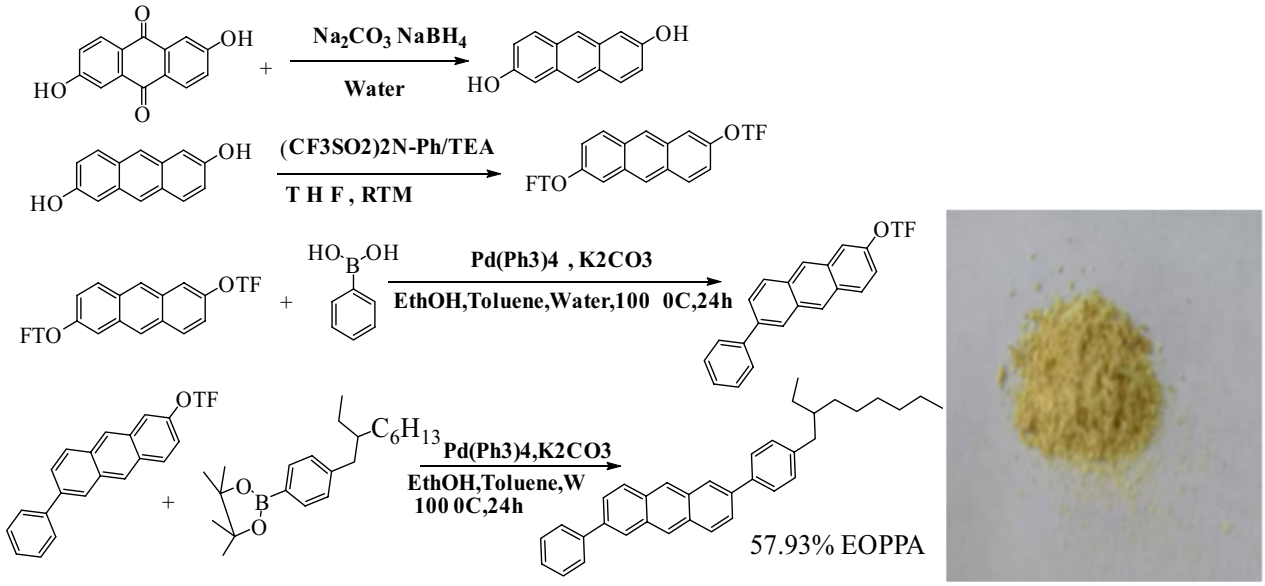

Scheme 1 Synthesis of EOPPA

Results and discussions

Synthesis

The synthesis of EOPPA is shown in Scheme 1. The final product is easily obtained in four steps with a high yield. All reagents and chemicals obtained commercially were used without purification. These reactions can be achieved by attacking the C2 position of OTF with phenylboronic acid and the C6 position of OTF with 6-(4-(2-Ethyl Octyl) Phenyl)-4,4,5,5-tetramethyl-1,3,2-dioxaborolane. This unique scheme of attacking the C6 (6-position) and C2(2-position) of the OTF structure has successfully improved EOPPA stability either in the ambient environment or in high thermal conditions.

Optical and thermal stability properties

The optical properties of the EOPPA compound were analyzed using UV–vis absorption spectroscopy in both solution and solid states. During UV–vis measurement, EOPPA was diluted in CH_2Cl_2 solvent (10^{-3}, 10^{-5} Molar), the vitality can be calculated from the material observed within the 300–700 nm range of the UV-visible machine. UV–vis spectrophotometry is commonly used in the quantitative chemical analysis of solutions. The distribution of electron density in EOPPA's highest occupied molecular orbital (HOMO) and lowest unoccupied molecular orbital (LUMO) are mainly concentrated on the central anthracene unit, with the presence of the alkyl group of one side chain. they are suggesting that the incorporation of phenyl and alkyl groups enhances the conjugation within the molecule. This improvement in molecular conjugation can be attributed to the specific spin angle between the substituents and the anthracene skeleton. The optimal alignment and orientation of these groups contribute to a more efficient delocalization of π-electrons, leading to enhanced electronic communication and extended conjugation throughout the EOPPA structure, as a result, The UV–vis retention range of EOPPA remained consistent at approximately 400 nm in both the solid-state and solution state, shown in Fig. 1a, b. UV–visible spectroscopy is a fascinating study of electronic energy.

The advancement and widespread adoption of organic transistors in emerging applications necessitate significant improvements in their stability. Thermal stability is a major concern because organic semiconductors break down or evaporate at lower temperatures than inorganic ones. The thermal stability of EOPPA is measured through thermal gravimetric analysis, which confirms its physiochemical properties. EOPPA weighs approximately 8.3 mg. The TGA instrument measures the mass of a sample as it's heated to cool and stabilize the material, which indicates that the EOPPA is stable under the ambient atmosphere and ensures its practical application. The weight of the EOPPA fabric exhibited minimal variation when the temperature was maintained below 300℃, indicating its stability under these conditions. We measured the thermal stability of EOPPA using TGA curves at temperatures of almost 225 °C (seen in Fig. 1C, Additional file 1: Fig. S2b). The EOPPA compound demonstrated a decomposition temperature (Td, 5% weight loss) of approximately 225 °C, indicating its thermal stability up

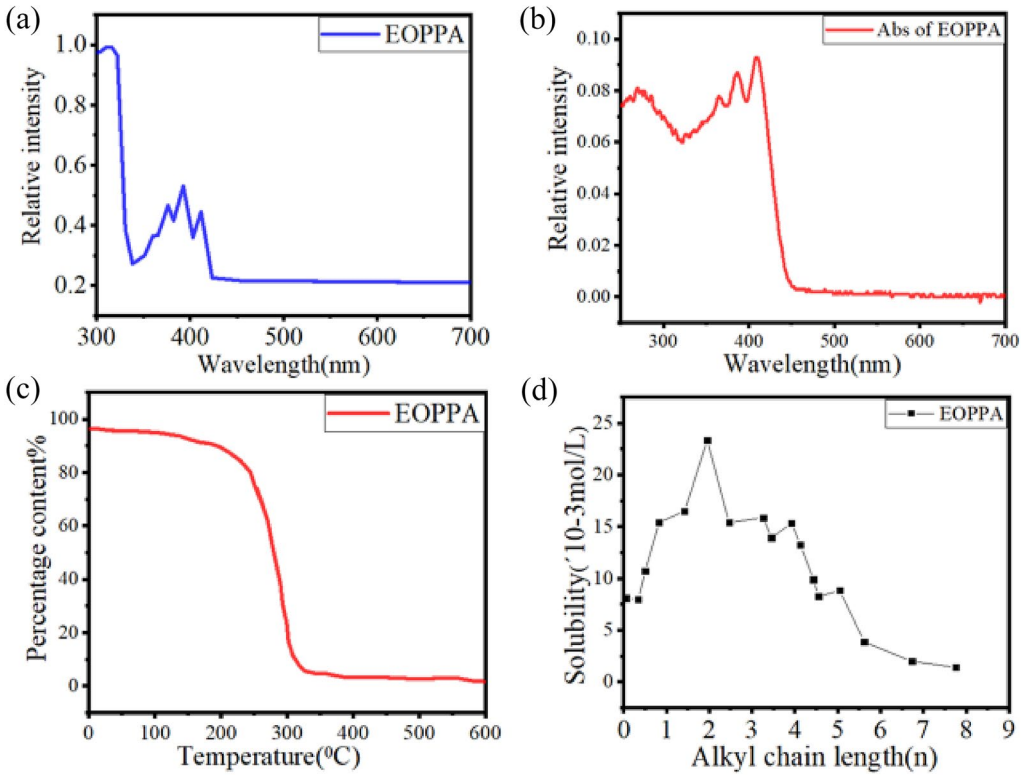

Fig. 1 **a** UV–vis absorption spectrum of EOPPA in a solution state, **b** UV–vis absorption spectrum of EOPPA in a solid state, **c** thermogravimetric analysis graph, and **d** solubilities spectrum

to this temperature threshold. The TGA results revealed that EOPPA exhibits exceptional thermal stability, as evidenced by its high decomposition temperature of approximately 225 °C. This finding underscores the robustness and strength of EOPPA as a molecule, showcasing its ability to endure and withstand elevated temperatures without significant degradation or weight loss.

The solubility and thermal properties of EOPPA were examined and plotted as a function of the alkyl chain. The result revealed intriguing trends, suggesting that as the alkyl chain, the solubility of EOPPA in solvent also exhibited a corresponding increase. This can be attributed to the enhanced intermolecular interactions and improved molecular packing facilitated by the alkyl chain, leading to improved solubility. Additionally, the thermal properties of EOPPA showed a notable pattern, with the alkyl chain generally correlating with enhanced thermal stability. This can be attributed to the increased steric hindrance and improved molecular rigidity imparted by the alkyl chain, which provides greater resistance to thermal degradation. Overall, the systematic exploration of solubility and thermal properties of the alkyl chain sheds light on the structural factors governing the performance and stability of EOPPA, thereby informing the design and optimization of future organic materials with tailored properties that can be understood based on structural variation All results indicate that the structural features dictate the solubility characteristics of the EOPPA compound (Fig. 1d), however, EOPPA dissolves easily in DCM and some organic solvents due to its one-sided alkyl chain effect.

Single-crystal structure

The crystal structure and molecular packing of EOPPA were analyzed to understand the impact of substituents on its structure. Advanced characterization techniques including XRD, SEAD, and TEM were employed for this comprehensive analysis.

The XRD was done with an angle of 5°–50°. The analysis of EOPPA using X-ray diffraction techniques provided valuable insights into its crystal structure. However, due to the molecular structure of EOPPA, which includes a side chain and a "tentacle-alkyl structure," the formation of a single crystal was inhibited. As a result, the X-ray techniques primarily revealed peak positions rather than providing detailed surface information. Nevertheless, the obtained narrow, intense, and sharp peaks in the XRD graph indicate crystallinity and excellent structural order within the EOPPA material. Despite the challenge of forming a single crystal, the presence

of these well-defined peaks suggests that EOPPA adopts a closed-packed arrangement in its molecular packing. This closed-packed structure is likely a result of the efficient packing of the EOPPA molecules, facilitated by the presence of a side chain and the tentacle-alkyl structure. Although the surface characteristics could not be directly determined through X-ray techniques, the observed peak features provide valuable insights into the overall quality and organization of the EOPPA material's crystal lattice. Eventually, the XRD analysis of EOPPA exhibited distinct characteristics, at 2Θ = 6.0, 12.50, and 19.0, while low-intensity peaks at 2Θ = 21.0 and 25.0. The XRD peaks indicate that EOPPA is a crystallized material (Fig. 2a).

The resolution TEM imaging of EOPPA provided further clarity regarding its crystal formation. The TEM images revealed that EOPPA does not exhibit the typical single crystal structure due to the presence of a "tentacle" at one end of its molecular structure. However, the images displayed the presence of a closely packed EOPPA crystal structure. Despite the absence of well-defined single crystals, the close-packed arrangement of EOPPA molecules within the crystal lattice was evident from the TEM observations. This suggests that EOPPA molecules efficiently pack together, forming a dense and ordered structure. The "tentacle" feature in the molecular structure may influence the packing behavior, leading to the observed close-packed crystal formation. The resolution TEM images provided valuable insights into the detailed morphology and packing arrangement of EOPPA, shedding light on its unique crystal structure and enhancing our understanding of its properties for potential applications. The SEAD and TEM images are shown in Fig. 2b. However, nanostructures synthesized from π-conjugated molecules have attracted specific intrigue as building squares for optoelectronic gadgets such as field-effect transistors and complementary inverters. Compared to Organic Thin Films, a single crystal can appear to have inherent charge-transport properties.

Further, morphological analysis was made via through optical microscope (OM) Additional file 1: Fig. S4, in OM crystalline silicon wafers were used as the sample substrate. The transparency and high atomic-plane structure of silicon wafers make them an excellent material for imaging small particles, the OM techniques suggested a Two-dimensional (2D) morphology structure of EOPPA packing-crystal which is shown in Fig. 2c. Optical image (transmitting mode) and the corresponding SAED pattern of an 800 μm Edge length of crystal monolayer EOPPA domains as a function of time shown in Fig. 2d, these islands have an EOPPA crystal structure

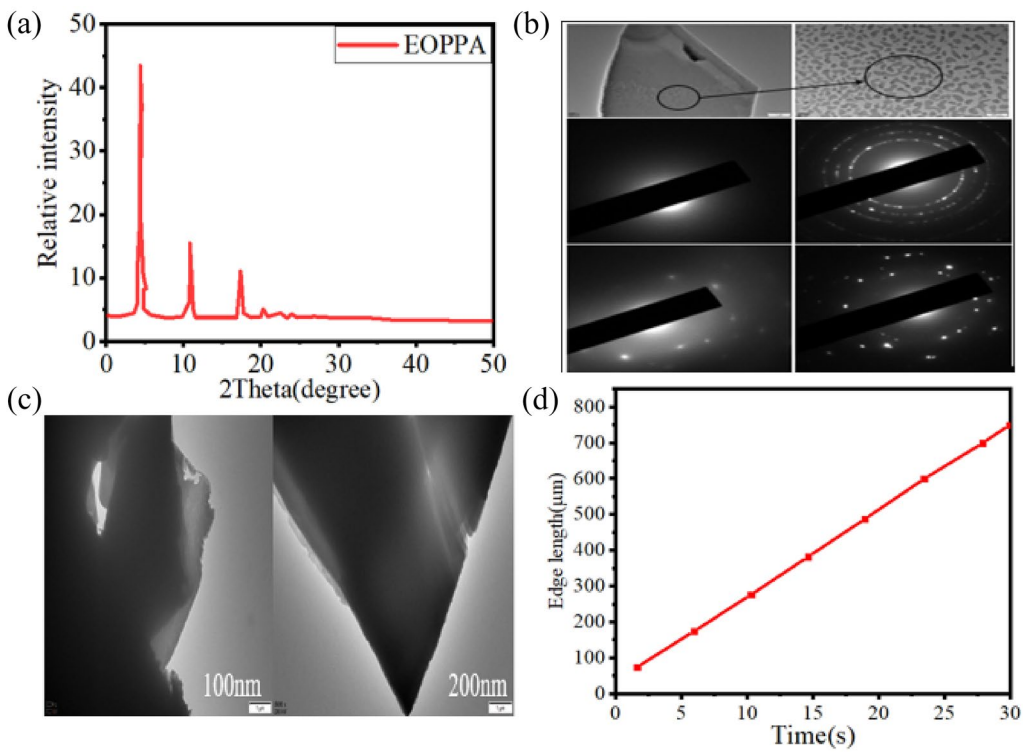

Fig. 2 **a** XRD spectrum of EOPPA. **b** TEM resolution images of EOPPA, **c** OM images of EOPPA, and **d** Edge length of crystal monolayer EOPPA domains as a function of time

with multi-layers, and the SAED cannot find a precise crystal atomic arrangement. In summary, the EOPPA is an organic semiconductor and crystalline material with a "tentacle-alkyl" structure of 3-Ethyl Octane, making it unsuitable for single crystals. This is why it has close-packed structures.

Charge transport properties of OFETs

To assess the charge transport properties of EOPPA, OTFTs were fabricated using 100 nm films in a "top-contact" geometry, as depicted in Fig. 3a. Remarkably, the EOPPA molecule consistently displayed a pronounced preference for adopting a slipped π–π stacking pattern, irrespective of variations in substrate conditions (whether OTS-modified or bare SiO_2/Si) and deposition parameters. This characteristic stacking arrangement indicates strong intermolecular interactions and efficient charge transfer within the EOPPA thin films. The observed stability in the slipped π–π stacking pattern across different substrates and the deposition conditions demonstrate the robustness and reliability of EOPPA as a material for achieving predictable charge transport behavior in OTFT devices. Many organic semiconductors exhibited multiple crystal phases (different molecular packing) when subjected to changes in substrates and deposition conditions, and their performance was significantly affected by these crystal phases. For this condition, we have synthesized and characterized EOPPA. In addition, we investigated and explored the charge transport abilities of EOPPA, which is a p-type organic semiconductor material. Later, vacuum-deposited copper Cu (3 nm thickness) strips were added onto a SiO_2 substrate to cover top-contact OSC/TFTs with the configuration and smooth deposition of EOPPA, the contact thickness of Au is 40 nm. At the same time, the channel width (W) and length (L) are 200 μm and 25 μm, respectively. In Fig. 3b, the photographic image of EOPPA indicates that its diffusion into the SiO_2 surface is even. Then, a shadow mask technique was utilized to create source and drain electrodes through the diffusion of EOPPA into a silicon wafer. The mobility tests were conducted on the complete system of devices under natural environmental conditions, providing valuable insights into the performance of the thin film devices in the air. The obtained output and transfer characteristics, depicted in Fig. 3c, d respectively, represent typical behavior for the EOPPA-based thin film devices.

To quantify the charge mobility, measurements were performed on the channel length and width along the direction of dip-coating. Remarkably, the calculated mobility values exceeded 0.18 $cm^2\ V^{-1}\ S^{-1}$ as shown in Figure Sa3, indicative of the excellent charge transport capabilities exhibited by the EOPPA thin films. Such mobility values are indicative of efficient charge carrier

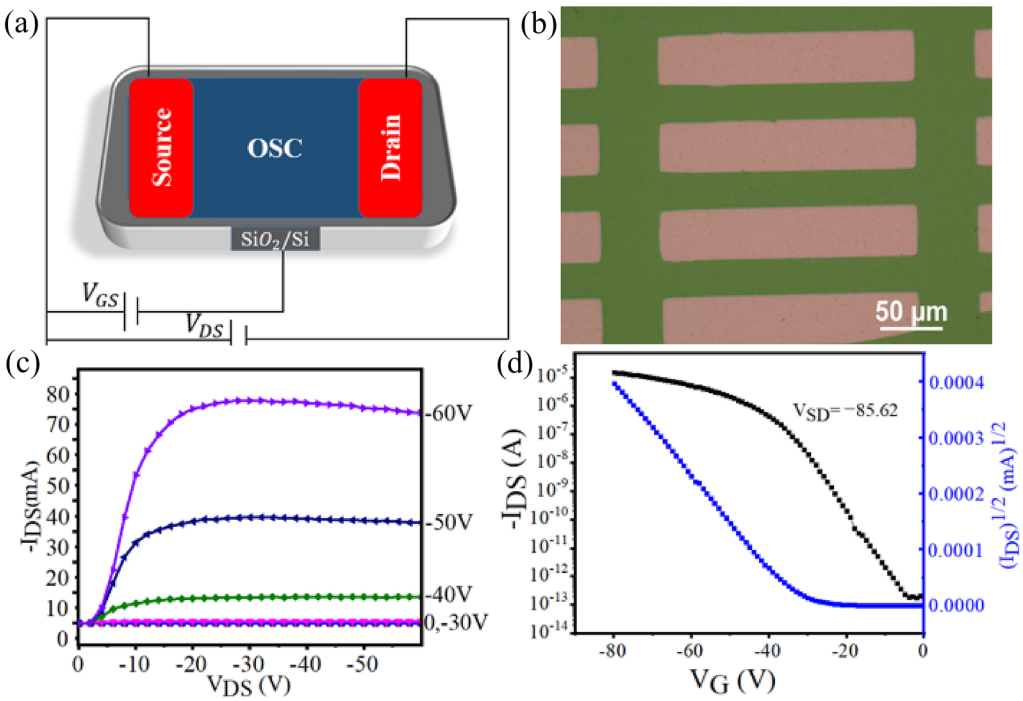

Fig. 3 **a** A schematic diagram of the OSC-FET. **b** The photographic image of an OFET device. The width and length of the channel are 200 μm and 25 μm, respectively. **c** Typical output, and **d** typical transfer curves of the OTFTs

transport within the organic semiconductor layer, suggesting the presence of well-ordered and highly conducting pathways for electron flow. These results highlight the promising potential of EOPPA as a candidate for organic transistor applications, particularly in the development of high-performance electronic devices. The observed good mobility values underscore the favorable charge transport properties of EOPPA, making it a promising material for the realization of efficient and reliable organic thin film transistors.

The EOPPA conductivity or charge transfer abilities can be measured through CV by calibrating the CV with ferrocene/ferrocenium (Fe/Fe+) as an external reference. To determine the HOMO and LUMO energy levels, refer to Additional file 1: Fig S2a. The HOMO energy level was estimated according to the onsets of the oxidative peaks and the empirical formula $E_{HOMO} = -\left(E_{ox}^{onset} + 4.8 + E_{Fe/Fe^{+}}^{onset}\right)$ eV. The LUMO energy level was calculated by using the bandgaps and the HOMO level ($E_{LUMO} = E_{HOMO} + Eg$), the energy difference between HOMO and LUMO is linked to wavelength by the equation Energy Difference = (h * C)/wavelength, where h is Planck's constant and C is the speed of light. Figure 4a displays the molecular structure of EOPPA, while Fig. 4b exhibits the CV curves of EOPPA in a dilute CH_2Cl_2 solution. In the CV analysis of EOPPA, the calculated HOMO level was determined to be approximately −5.138 eV. This value is notably 0.462 eV more negative compared to the HOMO level of DPA, which measures −5.6 eV [21]. The distinct HOMO levels of various DPVAnt derivatives, including EOPPA, are visually represented in Fig. 4b and Additional file 1: Fig S1T.

These findings highlight the variation in electronic structure among different DPVAnt derivatives, with EOPPA exhibiting a lower HOMO energy level compared to DPA. The difference in HOMO levels implies potential variations in the electronic properties and charge transport behavior of these derivatives. The precise control and understanding of the HOMO energy levels in DPVAnt derivatives, such as EOPPA, are crucial for tailoring their electronic properties and optimizing their performance in various applications, including organic electronics and photovoltaics. The provided figures offer a visual representation of the diverse HOMO energy levels within the DPVAnt derivative family, aiding in further analysis and exploration of their electronic structure-property relationships [18], this can be achieved by substituting the acenes with anthracene derivatives. The HOMO and LUMO orbitals of EOPPAs are shown in Fig. 4C, with energies of −5.138 eV and −1.779 eV, respectively. These findings offer an initial blueprint for creating organic semiconductors through a solution-based process. The molecular scheme of EOPPA requires further investigation due to low mobility results. According to this report, the mobility of the film is over 0.18 $cm^2 V^{-1} S^{-1}$, and a high current on/off ratio for the EOPPA film, it has been discovered that the presence of

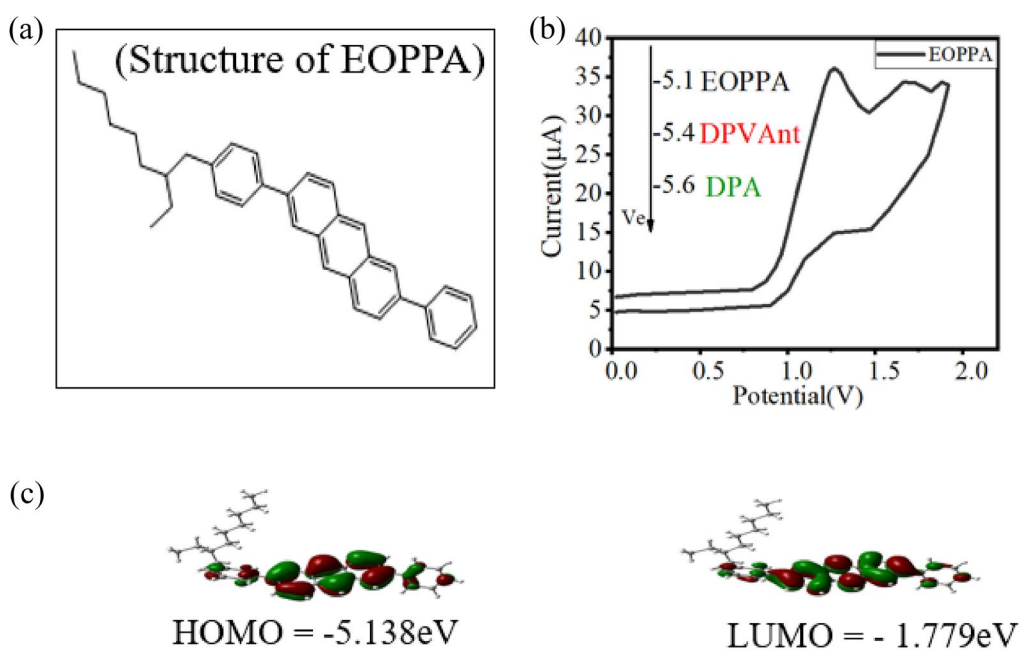

Fig. 4 **a** Molecular structure of EOPPA. **b** Cyclic voltammograms curves of EOPPA and HOMO levels of typical p-type semiconductor (inlet). **c** HOMO and LUMO orbitals enrage level for EOPPA

an alkyl chain on one side of the film adversely affects its mobility. This finding was made using a device structure commonly employed in solution-processing OTFTs. The influence of the alkyl chain on mobility suggests that the molecular arrangement and intermolecular interactions within the EOPPA film play a crucial role in determining its charge transport properties. Therefore, further investigation is necessary to elucidate the specific molecular factors governing the mobility behavior of EOPPA and explore strategies for enhancing its charge carrier mobility. Gaining a better understanding of the molecular structure and its effects on movement can lead to valuable insights. In the future researchers have the potential to optimize EOPPA's molecular design and develop improved materials for high-performance OTFT applications.

Conclusion

In summary, organic semiconductors have received a lot of research interest due to their extensive synthesis and structural variety, which enable molecular design to include various features. Thus, we have designed, synthesized, and characterized a side alkyl chain anthracene core new molecule as 6-(4 (-2 Ethyl Octyl) Phenyl) 2Phenyl Anthracene (EOPPA) p-type semiconductor. It was effectively synthesized with four basic steps and in excellent yield. EOPPA is an effective semiconductor compound inferred from a run of anthracene subordinates, The EOPPA has been obtained from an inexpensive source, and this compound can work as an actor for the run of p-type organic semiconductors in charge carriers. We have done the characterization of EOPPA such as thermal stability, solubility, crystal structure, and application of charge transfer. The arrangement's EOPPA's UV–vis assimilation rate was 400 nm, and its reliability temperature was almost 225 °C, all of the results indicate that the structural characteristics of the EOPPA compound control its solubilities and thermal characteristics. The EOPPA compound was considered a tough, tall-performing semiconductor with the versatility of a thin-film gadget over 0.18 $cm^2 V^{-1} S^{-1}$. The excellent performance and skillful arrangement-preparation combination of EOPPA show tremendous potential in organic electronics. In this study, we noted its inability to self-assemble into a single crystal, but it is suitable as a close-packed material. Eventually, we were able to create the new molecule, an anthracene derivative with a side alkyl chain, a p-type organic semiconductor with optoelectronic physicochemical characteristics, and close crystalline behaviors. Additionally, it offers useful direction for the design and synthesis of future organic semiconductors that will prove to be more successful.

Supplementary Information

The online version contains supplementary material available at https://doi.org/10.1186/s40486-023-00187-6.

Additional file 1: Schema S1. The first step of the reaction. **Schema S2.** The second step of the reaction. **Schema S3.** The middle molecule step. **Schema S4.** The final molecule step. **Table S1.** Summary of the properties of typical anthracene derivatives, especially EOPPA, compared to relative molecules. **Figure S1.** (a) ^{1}H NMR, and (b) MS (EI): m/z 471 (M+) results of EOPPA. **Figure S2.** Thermo gravimetric analysis and Cyclic Voltammeters curve (CV) of EOPPA. **Figure S3.** The photographic image of an OFET device, and typical transfer curves of EOPPA. **Figure S4.** OM images of EOPPA.

Acknowledgements

This work was supported by the National Natural Science Foundation of China (52121002). And also funded by the Fundamental Research Grant awarded by the Ministry of Higher Education Malaysia [FRGS/1/2019/STG07/UTHM/02/5 (FRGS K171)] and TIER 1 (H218) and GPPS (H423), awarded by University Tun Husain Onn Malaysia (UTHM), Malaysia. The authors express their appreciation to the Deanship of Scientific Research at King Khalid University, Saudi Arabia, for funding this work through a research group program under grant number RGP. 2/167/43. This research was funded by the Princess Nourah bint Abdulrahman University Researchers Supporting Project number (PNURSP2023R1), Princess Nourah bint Abdulrahman University, Riyadh, Saudi Arabia.

Availability of data

The data that support the findings of this study are available from the corresponding author upon reasonable request.

Declarations

Ethics approval and consent to participate

The research is not involving studies on human or their data.

Competing interests

The authors declare that they have no known competing financial interests or personal relationships that could have appeared to influence the work reported in this paper.

Received: 17 September 2023 Accepted: 19 November 2023
Published online: 15 December 2023

References

1. Wang C, Dong H, Hu W, Liu Y, Zhu D (2012) Semiconducting π-conjugated systems in field-effect transistors: a material odyssey of organic electronics. Chem Rev 112(4):2208–2267
2. Sirringhaus H (2003) An equal-opportunity conductor. Nat Mater 2(10):641–642
3. Mitzi DB, Kosbar LL, Murray CE, Copel M, Afzali A (2004) High-mobility ultrathin semiconducting films prepared by spin coating. Nature 428(6980):299–303
4. Reese C, Roberts M, Ling MM, Bao Z (2004) Organic thin film transistors. Mater Today 7(9):20–27
5. Horowitz G (2004) Organic thin film transistors: from theory to real devices. J Mater Res 19(7):1946–1962
6. Klauk H, Halik M, Zschieschang U, Schmid G, Radlik W, Weber W (2002) High-mobility polymer gate dielectric pentacene thin film transistors. J Appl Phys 92(9):5259–5263
7. Jones BA, Ahrens MJ, Yoon MH, Facchetti A, Marks TJ, Wasielewski MR (2004) High-mobility air-stable n-type semiconductors with processing versatility: dicyanoperylene-3, 4: 9, 10-bis (dicarboximides). Angew Chem-Int Ed 43(46):6363–6366

8. Meng H, Bao Z, Lovinger AJ, Wang BC, Mujsce AM (2001) High field-effect mobility oligofluorene derivatives with high environmental stability. J Am Chem Soc 123(37):9214–9215
9. Payne MM, Parkin SR, Anthony JE, Kuo CC, Jackson TN (2005) Organic field-effect transistors from solution-deposited functionalized acenes with mobilities as high as 1 $cm^2/V{\cdot}s$. J Am Chem Soc 127(14):4986–4987
10. Mas-Torrent M, Hadley P, Bromley ST, Vecianaa J, Roviraa C (2007) Organic field-effect transistors: tetrathiafulvalene derivatives as highly promising organic semiconductors. New Developments in nanotechnology research. Nova Science Publishers Inc, New York, pp 79–93
11. Mette H, Pick H (1953) Elektronenleitfähigkeit von anthracen-einkristallen. Z Phys 134(5):566–575
12. Van Damme J, Du Prez F (2018) Anthracene-containing polymers toward high-end applications. Prog Polym Sci 82:92–119
13. Aleshin AN, Lee JY, Chu SW, Kim JS, Park YW (2004) Mobility studies of field-effect transistor structures based on anthracene single crystals. Appl Phys Lett 84(26):5383–5385
14. Meng H, Sun F, Goldfinger MB, Jaycox GD, Li Z, Marshall WJ, Blackman GS (2005) High-performance, stable organic thin-film field-effect transistors based on bis-5′-alkylthiophen-2′-yl-2, 6-anthracene semiconductors. J Am Chem Soc 127(8):2406–2407
15. Ito K, Suzuki T, Sakamoto Y, Kubota D, Inoue Y, Sato F, Tokito S (2003) Oligo (2, 6-anthrylene) s: acene–oligomer approach for organic field-effect transistors. Angew Chem Int Ed 42(10):1159–1162
16. Merlo JA, Newman CR, Gerlach CP, Kelley TW, Muyres DV, Fritz SE, Toney MF, Frisbie CD (2005) P-channel organic semiconductors based on hybrid acene–thiophene molecules for thin-film transistor applications. J Am Chem Soc 127(11):3997–4009
17. Deng WQ, Goddard WA (2004) Predictions of hole mobilities in oligoacene organic semiconductors from quantum mechanical calculations. J Phys Chem B 108(25):8614–8621
18. Jiang L, Hu W, Wei Z, Xu W, Meng H (2009) High-performance organic single-crystal transistors and digital inverters of an anthracene derivative. Adv Mater 21(36):3649–3653
19. Meng H, Sun F, Goldfinger MB, Gao F, Londono DJ, Marshal WJ, Blackman GS, Dobbs KD, Keys DE (2006) 2, 6-Bis [2-(4-pentylphenyl) vinyl] anthracene: a stable and high charge mobility organic semiconductor with densely packed crystal structure. J Am Chem Soc 128(29):9304–9305
20. Dong Y, Guo Y, Zhang H, Shi Y, Zhang J, Li H, Lu X, Yi Y, Li T, Hu W, Jiang L (2019) Cyclohexyl-substituted anthracene derivatives for high thermal stability organic semiconductors. Front Chem 7:11
21. Liu J, Dong H, Wang Z, Ji D, Cheng C, Geng H, Zhang H, Zhen Y, Jiang L, Fu H, Bo Z, Chen W, Shuai Z, Hu W (2015) Thin film field-effect transistors of 2, 6-diphenyl anthracene (DPA). Chem Commun 51(59):11777–11779
22. Liu J, Zhang H, Dong H, Meng L, Jiang L, Jiang L, Wang Y, Yu J, Sun Y, Hu W, Heeger AJ (2015) High mobility emissive organic semiconductor. Nat Commun 6(1):10032

Publisher's Note